Improvement of main drift chamber Monte-Carlo tuning model at BESIII [*]

ZHANG Rui(张瑞)[1;1)]   XIAO Dong(肖栋)[2]   AN Fen-Fen(安芬芬)[2]   GAO Yuan-Ning(高原宁)[3]

HE Kang-Lin(何康林)[2]   JI Xiao-Bin(季晓斌)[2]   JIN Shan(金山)[2]   LI Wei-Dong(李卫东)[2]

LI Wei-Guo(李卫国)[2]   LIU Huai-Min(刘怀民)[2]   LIU Kai(刘凯)[3]   SHEN Xiao-Yan(沈肖雁)[2]

WANG Yi-Fang(王贻芳)[2]   WU Ling-Hui(伍灵慧)[2]   XU Qing-Nian(徐庆年)[1]   YUAN Ye(袁野)[2;2)]

ZHANG Yao(张瑶)[2]   ZHAO Guang(赵光)[2]   ZHENG Yang-Heng(郑阳恒)[1]

[1] University of Chinese Academy of Sciences, Beijing 100049, China
[2] Institute of High Energy Physics, Chinese Academy of Sciences, Beijing 100049, China
[3] Tsinghua University, Beijing 100084, China

Abstract: Based on real data, a new parameterized model of the main drift chamber response is proposed. In this model, we tune the ratio of good hits and the residual distribution separately. By data quality checking, the difference between simulation and data in track reconstruction efficiency reduces from 1% to 0.5% averagely for the pion in $J/\psi \rightarrow \pi^+\pi^-\pi^0$, and the momentum resolution agreement improves significantly for the proton in $J/\psi \rightarrow p\bar{p}$.

Key words: BESIII, main drift chamber, Monte-Carlo tuning, hit category

PACS: 29.40.Gx, 29.40.Cs, 13.66.Jn   **DOI:** 10.1088/1674-1137/38/2/026201

1   Introduction

The Beijing Spectrometer III (BESIII) [1], which operates at the upgraded Beijing Electron Positron Collider (BEPC II), consists of the following sub-detectors: Main Drift Chamber (MDC), Time of Flight Counter (TOF), Electromagnetic Calorimeter (EMC) and Muon Counter (MUC). The MDC is the core sub-detector, measuring the decay vertex, energy loss and momentum of charged particles precisely. There are 6796 sense wires with a positive high voltage (HV), most of which are surrounded by eight field wires. A drift cell is defined as the sensitive region of a sense wire. The whole MDC is in a 1.0 Tesla magnetic field provided by a super-conducting solenoid between EMC and MUC.

The MDC plays an important role in reconstructing charged tracks and identifying particles. A charged particle passing the drift cell ionizes the surrounding atoms of gas. The primary electrons drift towards the sense wire, being accelerated by the electric field in the drift cell and thereby initiating electron avalanches. These stripped electrons are eventually collected by sense wires and then produce electronic signals. If the magnitude of a signal exceeds a threshold value, relevant information

will be recorded by the electronic system. This fired wire is called a hit.

Since the first physics data taken in 2009, the peak luminosity of BEPC II has reached 7×10^{32} cm^{-2}·s^{-1}, which is about 70 times of BEPC. High luminosity and huge data sample reduce the statistical error of physical measurement significantly, and also call for a decrease of systematic uncertainty. A reliable Monte-Carlo (MC) simulation is important since event selection, efficiency calculation and background estimation in the physics analysis all rely heavily on it. Based on the GEANT4 [2] package, the BESIII Object Oriented Simulation Tool (BOOST) [3] was developed on the framework of the BESIII Offline Software System (BOSS) [4]. For physics analysis, good consistencies of tracking efficiency and momentum resolution between MC and data are crucial. In this letter, we describe a new method based on hits category to improve the MDC MC tuning (short for "tuning").

2   Tuning principles

The tracking efficiency is positively related to the raw hit efficiency, which is the probability of the sense wire firing when a charged particle passes though the drift

cell. The momentum resolution is mainly contributed by the intrinsic resolution and multiple scattering. The latter factor has been considered in GEANT4 package. The intrinsic resolution of MDC reflects the errors of particle position measurement. It contains the effects of primary ionization position, electron diffusion along the drift path, the amount and positions of avalanches and the distortion of the electric field at the edges of the drift cell. These processes are complicated for simulation from the first principle due to the limitation of computing power. The spatial resolution effect is composed of the intrinsic resolution contribution, multiple scattering, beam background, electronic noise and tracking algorithm.

Thus we build a parameterized model based on the raw hit efficiency and the spatial resolution for tuning. The values of parameters are extracted from the relevant distributions of real data. In order to get a better consistency, the iteration procedures are applied: using the model with initial values to generate a simulation sample and then comparing its relevant distributions with the real data's and adjusting the input values.

In practise, the spatial resolution is described by residual distribution. Therefore, raw hit efficiency and residual distribution are two key indicators when tuning.

3   Previous method

With the past experience from BES II [5], we find it difficult to obtain a consistency of the two key indicators simultaneously, by only tuning residual distribution. A better strategy is to tune the raw hit efficiency and the residual distribution separately [6].

3.1   Raw hit efficiency

The raw hit efficiency is given by:

$$\epsilon_\mathrm{H} = \frac{N_\mathrm{hit}}{N_\mathrm{pass}}, \qquad (1)$$

where N_pass is the number of drift cells passed by track; N_hit means the number of drift cells fired in N_pass. We use helix parameters given by a reconstruction algorithm to predict N_pass.

The ϵ_H is a function of cell position, the distance of closest approach (DOCA) and dip angle. So we divide it into three parts: ϵ_cell, ϵ_doca and $\epsilon_{\cos\theta}$ and tune them separately.

3.2   Residual distribution

The residual of a hit is defined as:

$$r = d_\mathrm{drift} - d_\mathrm{doca}, \qquad (2)$$

where d_drift is the drift distance of the hit, calculated by drift time and distance-time relation (X-T relation);

the DOCA, d_coca, is calculated by the parameters of the helix–which are obtained from the other hits on this track.

The residual distribution depends on layer, DOCA and entrance angle. Thus, all hits are categorized by different layers, DOCA and entrance angles; we tune each residual distribution one by one. Double-Gaussian is used to describe the residual shape of a signal; a 2-order Polynomial is employed to describe the shape of background and noise. In simulation, the contribution of beam background has been considered by random background sampling. Thus the polynomial part will not be tuned. As a result, there are five parameters for the residual distribution: $(f, \mu_1, \sigma_1, \mu_2, \sigma_2)$, in which f stands for the fraction of the first Gaussian; μ_1, μ_2 stands for the mean values of the two Gaussians; and σ_1, σ_2 stands for the standard deviations.

3.3   Limitation and discussion

In the previous method, the average of tracking efficiency difference could be reduced to 1%. Further comparison shows that a part of residual distributions near the sense wire has a tail at the positive side, especially in inner layers.

The residual tends to be positive due to its definition (Eq. (2)). As shown in Fig. 1, typically, d_doca will not be larger than d_drift. This kind of discrepancy is enlarged in inner layers, where a lower working voltage than designed is applied to protect the detector from the high level of background. It requires more primary ionization to
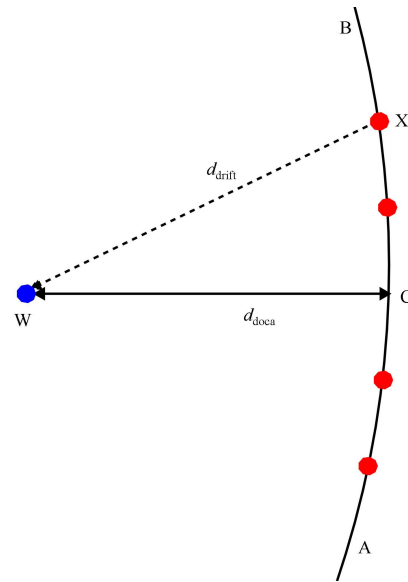

Fig. 1. A schematic diagram of residual. W is a sense wire. A particle flies along $\overparen{\mathrm{AB}}$. $\overline{\mathrm{WC}}$ is DOCA. Solid dots on $\overparen{\mathrm{AB}}$ are the positions of primary ionization. Suppose that X triggers the electronics. $\overline{\mathrm{WX}}$ is always longer than $\overline{\mathrm{WC}}$.

trigger the electronics. This could make X farther from C. As a result, the residual could be much larger.

In order to verify the judgement, we select electron tracks from a Bhabha sample, which is colleced with full high voltage on inner layers. In Fig. 2, plot (a) is the inner layer with a normal voltage. Plot (b) is the inner layer with full voltage. We also put an outer layer residual shape with full voltage as a reference (plot (c)). The conclusion is that with lower voltage on the wire, the tail tends to include more signal hits and, since these hits have no relationship with the beam background, they cannot be taken into account in either previous tuning or random background sampling.
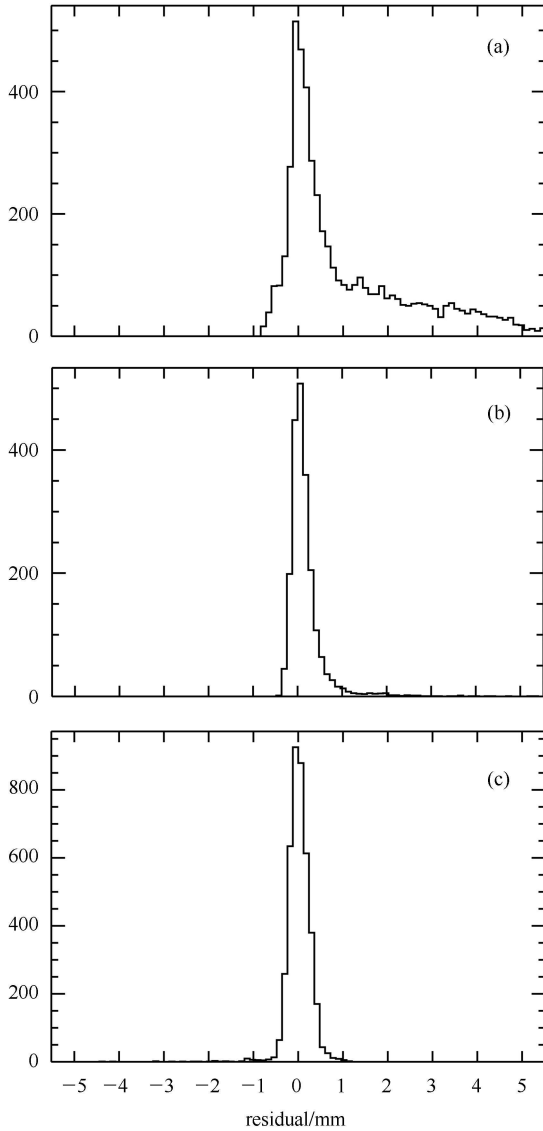

Fig. 2.   Residual distributions. Plot (a) is the inner layer with lower HV — the tail contains signals with large residual; (b) is the inner layer with full HV — the tail diminishes; (c) is the outer layer with full HV.

4   New method

In order to improve the agreement between data and MC, a new method is developed to consider those signals with relatively larger residual.

4.1   Hits category

The residual distribution is obtained by a track reconstruction algorithm [7, 8]. The reconstruction algorithm drops those hits which make a large contribution to χ^2 when fitting. As a result, the quality of a track is dominated by the hits adopted. In the previous method, we tune all hits as a whole. However, the consistency of the five parameters of the double-Gaussian does not necessarily ensure the agreement of the residual resolution of the hits on track.

A natural way of classification of all hits is based on whether a hit is used by the tracking reconstruction: the hits used eventually on track are good hits while those not used on track are bad hits.

The good-hit efficiency should be one of the criteria of the track quality. It is defined as:

$$\epsilon_{\mathrm{ghit}} = \frac{N_{\mathrm{ghit}}}{N_{\mathrm{pass}}}, \tag{3}$$

where N_{ghit} is the number of good hits; N_{pass} is the same as in Eq. (1). In the previous method, getting a better consistency of the good-hit efficiency requires a broadening or shrinking of the shape of the double-Gaussian. This will change the good hits residual distribution. Thus it is difficult to reduce the disagreement between simulation and data further.

4.2   Revised model

Since the raw hit efficiency is tuned before residual distribution, we retain the model of the raw hit efficiency, but rebuild a model of the residual distribution. We use a parameter, Ratio, to describe the proportion of good hits, a double-Gaussian function with five parameters (two means, two standard errors and a fraction) to describe the residual distribution of good hits, and a uniform distribution of large residual to describe the shape of bad hits.

Because a new parameter, Ratio, is introduced, the double-Gaussian only focuses on good hits distribution. This not only reduces the impact on good-hit efficiency, but also makes the fitting easer since the shape becomes better (Fig. 3).

4.3   Tuning procedures

The process of tuning raw hit efficiency stays the same as the previous method. After that, we tune the residual distribution. Due to the complicated correlation among the parameters, we make an order by their sen-

sitivity. The Ratio is tuned before the double-Gaussian shape.

4.3.1 Obtaining the initial values

We get the initial values of the six parameters from the residual distribution of real data. The Ratio is calculated by counting the numbers of good and total hits (Fig. 3(a)). The other five parameters are obtained by fitting the good hits distributions (Fig. 3(b)).
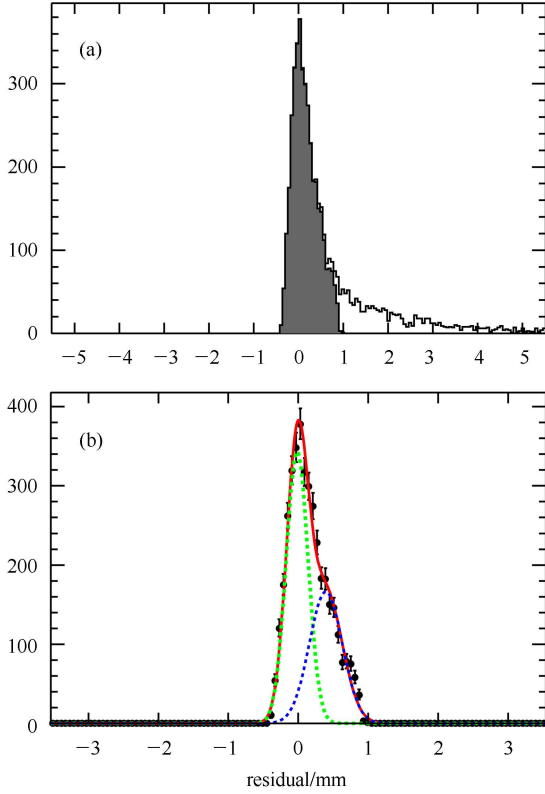

Fig. 3. (a) Two hit components: good hits (shaded) and bad hits (blank); (b) fitting result of good hits distribution by double-Gaussian.

4.3.2 Ratio tuning

We generate a MC sample by these initial values and compare the value of Ratio with the real data's. Based on the discrepancy, we change the input value while keeping the other parameters fixed.

4.3.3 Double-Gaussian identification

In order to decide which μ or σ should be modified, it is necessary to judge which Gaussian describes the certain part of the shape. Since σ is changing during tuning, we use h as the identifier:

$$h = f/\sigma, \qquad (4)$$

where f is the fraction of the Gaussian and σ is the standard error. The Gaussian with larger h is labeled as g_1 and the other one is g_2.

4.3.4 Gaussian shape tuning

The most sensitive parameter of the double-Gaussian is σ_1 since g_1 plays a main role in the residual distribution. After several iterations, the main part of the residual shape keeps consistent. Then we tune σ_2, f, μ_1 and μ_2 in sequence.

4.3.5 Tuning performance

We compare the raw hit efficiency and good-hit efficiency with real data after tuning, respectively (Fig. 4). After tuning, the efficiencies of MC and data agree well.
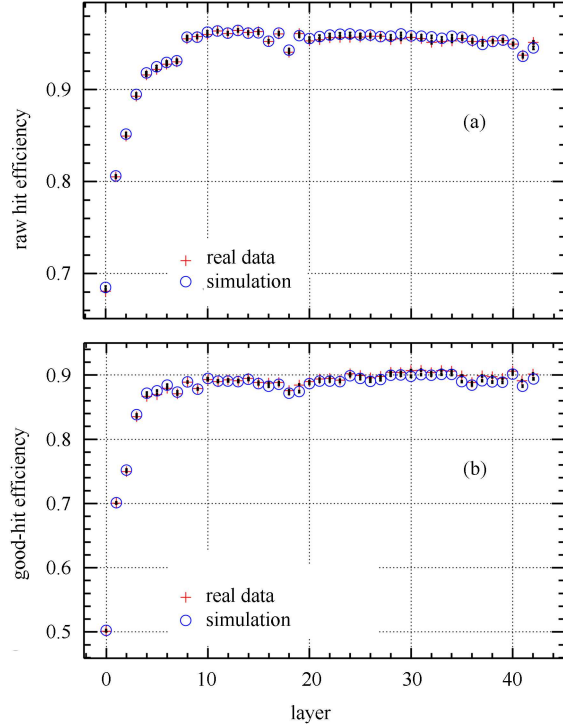

Fig. 4. Tuning results and comparisons to data. (a) Raw hit efficiency in each layer; (b) good-hit efficiency in each layer.
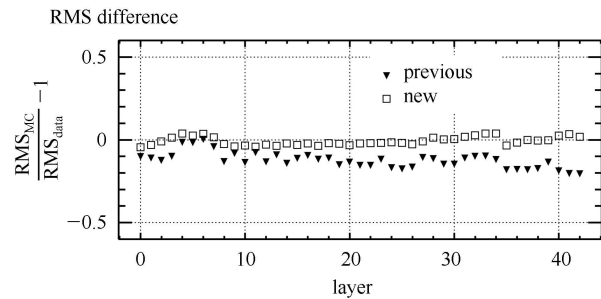

Fig. 5. RMS difference between MC and data. Full triangles down stand for the previous method and open squares stand for the improved method.

We also compare the difference of root mean square (RMS) of residual distribution in the two method in each

layer (Fig. 5). After the improvement, the difference between MC and data become much smaller.

5   Check with physics objects

In order to test the new method, we pick out some typical physics channels to compare results from simulation and real data.

5.1   Tracking efficiency

We use π from $J/\psi \to \pi^+\pi^-\pi^0$ to check the difference of tracking efficiency. Tracking efficiency is defined as:

$$\epsilon = \frac{N_{\text{found}}}{N_{\text{recoi}}}, \tag{5}$$

where N_{recoi} is the number of events in which π^0 and tagged charged pion have been reconstructed and the recoiled mass falls in the region of π; N_{found} is the number of events from N_{recoi} in which the recoiled π is reconstructed successfully. Fig. 6 shows that the difference of tracking efficiency between MC and data is about 0.5% averagely.
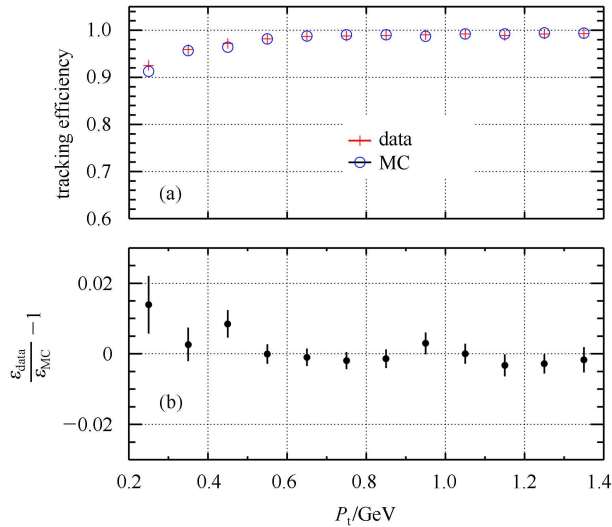

Fig. 6.   The tracking efficiency of π from $J/\psi \to \pi^+\pi^-\pi^0$. (a) Tracking efficiency in different transverse momentum and (b) efficiency difference.

Table 1.   Momentum resolutions for data and MC. The difference decreases significantly.

	previous/MeV	new/MeV
σ_{data}	7.827±0.013	7.827±0.013
σ_{MC}	7.097±0.011	7.639±0.035
$\frac{\sigma_{\text{MC}}}{\sigma_{\text{data}}}-1(\%)$	−9.33±0.21	−2.40±0.48

5.2   Momentum resolution

Protons from $J/\psi \to p\bar{p}$ are used to check the difference of momentum resolution. Fig. 7 shows the momentum distributions of the proton. The resolutions are listed in Table 1. The new method has a significant improvement.
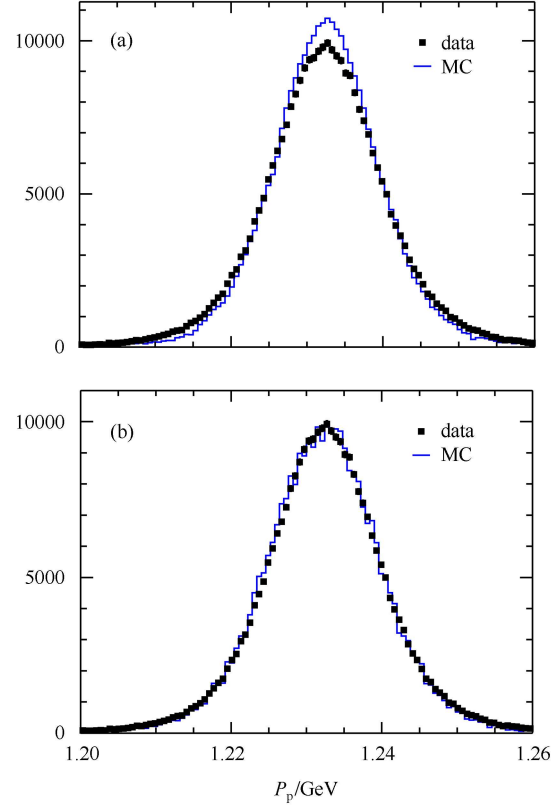

Fig. 7.   The momentum resolutions of proton. (a) The previous method and (b) the new method. Black dots are data and histograms are MC.

6   Summary

In this work, we noticed that signals could also cause large residuals. We employed a new category of hits and revised the model of residual distribution, which focuses on the good-hit efficiency and good hits residual shape directly.

Several advantages of the new method include:

1) Describing the real data better by splitting MDC hits into good and bad hits.

2) Reducing the correlation of good hits efficiency and spatial resolution, which is helpful to get better agreements of the tracking efficiency and momentum resolu-

tion at the same time.

3) Accelerating the process of tuning by using an efficient double-Gaussian identifier.

Using the new method, the differences in track reconstruction efficiency and momentum resolution decrease significantly. In the future, more effort should be devoted to understanding the asymmetry near the sense wire and finding a better model to describe it. Also, the discrepancy of tracking efficiency at low momentum is relatively larger. Thus we should try to improve the agreement for low momentum tracks. If necessary, further improvement can be developed to consider other effects, such as electronic field leakage, dE/dx and so forth.

References

1　Ablikim M et al. (BESⅢ collaboration). Nucl. Instrum. Methods A, 2010, **614**(3): 345–399
2　Agostinelli S, Allison J, Amako K et al. Nucl. Instrum. Methods A, 2003, **506**(3): 250–303
3　DENG Zi-Yan et al. HEP & NP, 2006, **30**(05): 371–377 (in Chinese)
4　LI W D, LIU H M, DENG Z et al. Proceeding of CHEP, 2006
5　Ablikim M, BAI J Z, BAN Y et al. Nucl. Instrum. Methods A, 2005, **552**(3): 344–356
6　LIU Kai et al. Nuclear Electronics & Detection Technology, 2012, **32**(9): 1012–1018 (in Chinese)
7　ZHANG Yao, ZHANG Xue-Yao, LI Wei-Dong et al. HEP & NP, 2007, **31**(06): 570–575 (in Chinese)
8　LIU Qiu-Guang, ZANG Shi-Lei, LI Wei-Guo et al. Chinese Physics C (HEP & NP), 2008, **32**(07): 565–571